MAUSAM, **77**, 1 (January 2026), 283-300

MAUSAM

DOI: https://doi.org/10.54302/0816t711
Homepage: https://mausamjournal.imd.gov.in/index.php/MAUSAM

UDC No. 551.509 .313.4:551.524(540)

Coupled model based operational extended range forecast of temperature over India during winter season of 2020-2021

Ashish Alone[1, 2], D. R. Pattanaik[2], Praveen Kumar[3], Anoop Kumar Shukla[1]

[1]*Department of Mechanical Engineering, Amity University Uttar Pradesh, Noida, India – 201313*

[2]*India Meteorological Department, Ministry of Earth Sciences, Lodi Road, New Delhi, India – 110003*

[3]*Regional Meteorological Centre, India Meteorological Department, Nagpur, Maharashtra, India – 440005*

(*Received 10 October 2024, Accepted 15 April 2025*)

***Corresponding author's email: ashishnalone@gmail.com**

सार – आईपीसीसी (2007) के अनुसार वर्ष 2050 तक जल उपलब्धता में 10-30% तक की कमी आने की संभावना है, जिससे मीठे पानी की गंभीर कमी उत्पन्न हो सकती है। मध्य महाराष्ट्र एक मौसम विज्ञान उप-विभाग है, जहाँ प्रमुख रूप से नकदी फसलों एवं अनाज फसलों की खेती की जाती है। हाल के वर्षों में इस क्षेत्र में अत्यधिक वर्षा की घटनाएँ दर्ज की गई हैं, जिसके कारण वर्षा परिवर्तनशीलता के अध्ययन की आवश्यकता उत्पन्न हुई।अतः वर्तमान अध्ययन में 1901 से 2020 की दीर्घकालीन वर्षा प्रवृत्तियों का विश्लेषण पारामीट्रिक एवं अपरामीट्रिक तकनीकों के माध्यम से किया गया। अध्ययन से यह पाया गया कि 1926 के बाद की अवधि में मध्य महाराष्ट्र उप-विभाग में वार्षिक वर्षा में बढ़ती हुई प्रवृत्ति देखी गई। यद्यपि चयनित सभी जिलों में मॉनसून वर्षा में वृद्धि की प्रवृत्ति दर्ज की गई, परंतु उनमें से केवल तीन जिलों (30%) में यह वृद्धि सांख्यिकीय रूप से महत्वपूर्ण पाई गई।इसके विपरीत, सांगली को छोड़कर लगभग सभी अध्ययन किए गए जिलों में शीतकालीन वर्षा में कमी देखी गई। इनमें धुले, अहमदनगर, पुणे एवं कोल्हापुर जिलों में वर्षा में गिरावट सांख्यिकीय रूप से महत्वपूर्ण रही। सभी समय पैमानों (मासिक, मौसमी एवं वार्षिक) पर महत्वपूर्ण परिवर्तन बिंदु (चेंज बिंदु) पाए गए। दस में से छह जिलों में पिछले पाँच वर्षों के दौरान परिवर्तन बिंदुओं का पंजीकरण हुआ। 2100 तक के भविष्य प्रक्षेपण से यह संकेत मिलता है कि इस क्षेत्र में वर्षा की मात्रा एवं परिवर्तनशीलता दोनों में संभावित वृद्धि हो सकती है। अतः इस अवलोकन से यह प्रश्न उत्पन्न होता है कि आने वाले दशकों में इन जिलों में वर्षा की स्थिति कैसी होगी और यह मध्य महाराष्ट्र उप-विभाग की समग्र वर्षा प्रवृत्ति को किस सीमा तक प्रभावित करेगी। साथ ही, अंतः-मौसमी एवं अंतः-ऋतु (इंटर एवं इंट्रा सीज़नल) वर्षा के बदलते स्वरूप पर भी आगे के अनुसंधान की आवश्यकता है, क्योंकि इसका प्रभाव मौसमी या अल्पकालिक फसल प्रतिरूप पर पड़ सकता है।

ABSTRACT. Agriculture, health, transportation, and hydrology are among the many sectors that rely significantly on intra-seasonal temperature fluctuations during the winter. The intra-seasonal variability of minimum (T_{min}) and maximum temperature (T_{max}) is observed across India during the winter season of November to February (NDJF). This study analyse the real time extended range forecast (ERF) skill of T_{min} and T_{max} over India during the winter season, *i.e.* NDJF of 2020-2021, using the Climate Forecast System version 2 (CFSv2) coupled model, operational in the India Meteorological Department. The statistical metrics, such as forecast accuracy, bias, probability of detection (POD), false alarm ratio (FAR), probability of false detection (POFD), critical success index (CSI), and the equitable threat score (ETS), are used to assess the temperature forecasting capability. A four-week quantitative comparison of observed and models predicted T_{min} is carried out, utilising every Wednesday's initial condition as the starting point. Throughout central India and northwest India, the intra-seasonal variability of observed T_{max} and T_{min} revealed a considerable reduction and rise in temperature over the winter season, with T_{min} fluctuation showing greater variability than T_{max} variability. The trend and intra-seasonal variations in T_{max} and T_{min} over India were well reflected in the real time extended range forecast during the season, up to 2 to 3 weeks. In a homogeneous region, northern and central India have higher skill levels than the southern peninsula and northeast India. At the district level in central and northwest India, categorical and quantitative forecasting ability was also found to be much more significant. As a result, for applications in various industries, the operational ERF of T_{max} and T_{min} with a lead time of 2 to 3 weeks may provide a reliable forecast.

Key words – Extended range forecast (ERF), Climate forecast system version 2 (CFSv2), Intra-seasonal variability, Cold wave, Minimum temperature.

1. Introduction

During the winter season, significant weather phenomena occur in the northwest and central parts of India associated with the passage of western disturbances (Dimri *et al.,* 2015; Midhuna *et al.,* 2020). A western disturbance occurs when moisture-laden winds replace cold and dry north-westerly winds with warm and moist easterly breezes. The Mediterranean is the source of western disturbances and cold waves, which ultimately migrate eastward into north India and higher terrains. As a result, they bring not only rain but also foggy and severe cold wave conditions to the country's north and north-eastern regions. Cold waves in India are occasionally caused by the north-south passage of winds from Siberia towards the equator. The major part of India is affected by a dry cold wind from the north, resulting in the formation of a cold wave (Dimri and Chevuturi 2016; Joseph *et al.,* 2019). Cold weather spells can be experienced throughout the Northwest and Central parts of India from November to February (NDJF). During the winter season, the passage of western disturbances, intense snowstorms in the Himalayan region, and the rainfall connected with them can be noticed (Lang and Barros 2004). The cold weather had arrived early over northern India in the winter season for 2020-21 of the year 2021, as strong winds swept in from the northwest, causing a moderate to severe winter, indicating the La-Nina impact, lowering temperatures (Zhang and Kumar, 2024). As a result of La-Nina, sea surface temperatures in the eastern and central Pacific Ocean were below normal, which impacts India as it brings the wind from northern Asia, particularly Siberia, into the country.

Considering the local climatic conditions, the India Meteorological Department (IMD) defined the cold waves and severe cold waves based on the threshold values (Rajeevan *et al.,* 2023). The cold wave condition is defined when the minimum temperature is less than or equal to 10 °C and simultaneously the departure is -4.5 °C to -6.4 °C, while said to be a severe cold wave when a similar condition exists for T_{min} and departure is -6.5 °C or less (for the plane region). Different studies were performed on the cold wave climate, its frequency and its persistence (Bedi and Parthasarathy 1967; Raghavan 1967; Subbaramayya and Rao 1976; Samra *et al.,* 2003). In India, these cold weather conditions are generally experienced during the period from November to February, NDJF.

As per the April 2023 IMD report, regions in northwest and central India reported the longest cold wave periods, lasting 10 days or more. Notably, Jammu and Kashmir endured the lengthiest cold wave period, lasting 18 days, while Bikaner and Jodhpur in western Rajasthan experienced a 16-day cold wave period. Additionally, Maharashtra witnessed cold wave periods exceeding 8 days. The majority of stations reporting cold wave periods of 5 days or more were situated in North, Northwest and Central India. Conversely, regions such as Kerala, coastal Karnataka, Tamil Nadu, and coastal Andhra Pradesh experienced fewer than 2 cold wave days per season. Since 2016, there has been an increase in the number of cold wave frequencies, raised from 2 to 5, particularly in northern regions where the maximum cold wave days increased from 4 to 5.

According to the climate diagnostic bulletins published by IMD (https://rcc.imdpune.gov.in/products.php), since 1901, during the winter of 2020-21 the mean temperature over India was 21.43 °C and remained third highest behind 2016 (21.8 °C) and 2009 (21.59 °C). Similarly, the T_{min} over all of India was 15.39 °C, after the year 2016. During the winter season of 2020-21, cold weather conditions were mostly moderate throughout central, western, and sections of eastern India in January, while cold wave conditions were mostly noted in the second half of the month (January) in northern India. During the first two weeks of February, there was a spell of cold wave that lasted for two days. According to the IMD, the average monthly T_{min} in northwest India in January 2021 was lower than in 2019 and 2020. However, average monthly maximum temperatures were 2° to 4 °C below normal in the Indo-Gangetic plain, as well as in regions of south Punjab and north Haryana to the west in January 2021. Several studies have indicated a significant increase in cold wave days over the Northwest India homogeneous region during the post-monsoon and winter seasons (Bhatla *et al.,* 2016; Gupta *et al.,* 2018). A study indicates a consistent rise in the frequency of cold wave days since 2017 (Ray *et al.,* 2021). The country saw 63 days of cold waves in 2018, which climbed by 1.5 times to 103 days in 2019. India experienced 99 days of cold waves in 2020, as per IMD reports. During the 2020-21 winter season, many parts of central and northwest India witnessed cold waves and severe cold wave conditions, particularly during the 2nd week of November, 2020; 3rd week of December, 2020 and also towards the end of January and beginning of February, 2021. This cold period has the potential to reduce crop yields, as well as have negative consequences for agriculture, livestock, and human health (Samra *et al.,* 2003). It has an impact on energy consumption, the ecosystem, and biodiversity as well. Human mortality due to cold waves was 76 times higher in 2020 than those due to hot waves. Cold waves

claimed 152 lives in 2020, compared to just two deaths from heat waves (NSO 2021).

Recently, IMD has implemented a coupled modelling system for the operational extended range forecast (ERF) based on the CFSv2 coupled model (Pattanaik *et al.,* 2019, 2020). The ERF of air temperature (hereinafter temperature) up to 3 to 4 weeks has numerous applications in sectors like agriculture, energy, health, insurance, power *etc*. Heat and cold wave forecasting with high accuracy can save lives and avoid property damage from these catastrophic weather events. The ERF also shows promising results in providing useful guidance for the heat and cold waves during summer and winter, with a statistically significant correlation coefficient (CC) for up to two weeks (Pattanaik 2015; Pattanaik *et al.,* 2019). As documented by earlier studies, operational ERF at homogeneous regions and sub-division level shows reasonable skill in predicting rainfall during the monsoon season (Pattanaik and Sahai 2018; Mandal *et al.,* 2019; Pattanaik *et al.,* 2019). It is observed that, many studies have been carried out to evaluate the skill of ERF at all India levels and also at meteorological scales, particularly for the monsoon rainfall during southwest monsoon season (Pattanaik *et al.,* 2021, 2022) at district level scale and also the heat wave during the summer monsoon season (Pattanaik and Sahai 2018; Joseph *et al.,* 2019) on sub-divisional scale. However, in order to fill the void for the precise ERF skill forecasting over the smaller spatial district domain for T_{min} forecast, a separate study will be more beneficial for the user or different stakeholder's communities. The present study deals with the real time skill performance analysis for the extended range forecast during the winter season from November 2020 to February 2021. The study analyses the quantitative forecast skills over the homogeneous Indian regions and sub-divisions along with the categorical skill forecast over the smaller spatial domain at district level over India.

2. Model data and the methodology

2.1. *Model data*

The current research aims to evaluate the performance of the National Centre for Environmental Prediction's (NCEP's) CFSv2 coupled model (Saha *et al.,* 2014), presently operational in IMD, in predicting the cold and extreme cold waves during the winter season of 2020-2021, covering the months of November, December, January and February (NDJF). The current study considers the month of NDJF, as most of the cold waves and severe cold waves over India occur during these months. A suite of models from the CFSv2 has been implemented in IMD. A total of four ensemble members, CFSv2 at T382 with horizontal resolution of around 38 km, CFSv2 at T126 with spectral triangular truncation of 126 waves and horizontal grid resolution of 100 km, GFSbc a Global Forecast System model version 2 (GFSv2) forced with bias corrected daily SST (bias-corrected SST from GFSv2) at T382 (~38 km), and GFSbc at T126 (~100 km), are run operationally for the period of thirty-two days based on the initial condition of every Wednesday. Subsequently, mean and anomaly forecasts on every Thursday are prepared, which are valid for four weeks (Friday to Thursday) for days 02-08 (week 1), days 09-15 (week 2), days 16-22 (week 3), and days 23-29 (week 4). The model used for the average ensemble forecast anomaly of all the four sets of model runs of 4 members each for 18 years of hindcast climatology. Ensemble members derived from different resolutions are weighted on their respective skill levels. The statistical method, Bayesian model averaging, is employed to optimize the combination of forecasts from different resolutions, considering their strengths and weaknesses. The day one forecast is excluded in the operational analysis as it takes time to accomplish the model integration (multi-model ensemble) and the generation of customised products for different sectorial applications. The mean correction method suggested by Richardson (2001) is utilized for the bias-corrected maximum temperature (T_{max}) and minimum temperature (T_{min}) of 1°×1° output data obtained from averaging ensemble outputs. The dataset covers the Indian mainland and has a resolution of 1°×1° same as of averaging ensemble model output. The formulation can be given as

$$\sum_{i=1}^{n} F_i - \sum_{i=1}^{n} O_i \quad (1)$$

where, F_i denotes the forecasted temperature and O_i denotes the observed temperature. The model outputs are assessed in comparison to daily observed T_{max} and T_{min} of the India Meteorological Department (IMD) available at the spatial resolution of 1°×1° (Srivastava *et al.,* 2009). This study uses the climatological normal from 1981-2010 for T_{max} and T_{min} from the observed data over the Indian land area at 0.5°×0.5° resolution.

2.2. *Methods*

A comprehensive study is performed on India's homogeneous meteorological regions, which have different meteorological subdivisions and include the districts of India, as shown in Fig. 1. The T_{max} and T_{min} gridded data in observation and model outputs are available at a coarser resolution and possibly very few grid points fall at the district level (lesser spatial extent) as compared to met-subdivisions and homogeneous regions. To overcome this challenge, a bilinear interpolation technique is applied to re-grid the observed and model data at finer spatial resolutions of 0.125°×0.125° to cover all the 676 districts of variable sizes spreading over India

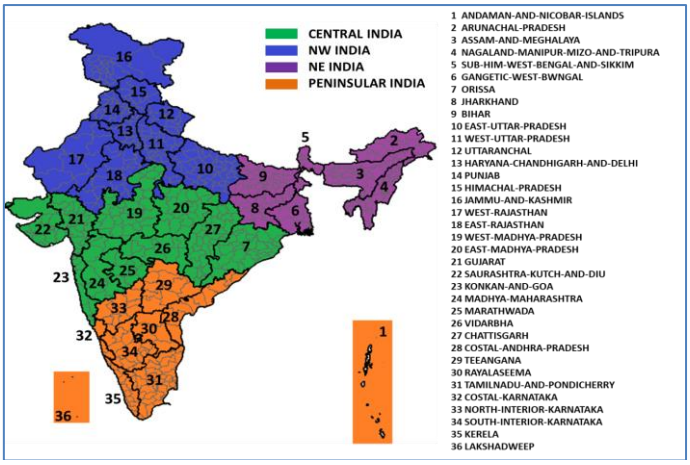

Fig. 1. Meteorological homogeneous regions, sub-divisions and districts in India

(Fig. 1). The method of bilinear interpolation can be obtained in the following manner (Andrews and Patterson 1976).

Let, $G(x_0, y_0)$, $G(x_1, y_0), G(x_0, y_1)$ and $G(x_1, y_1)$ be the four points over the rectangular grid (with coarser resolution) data as shown in Fig. 2. To obtain the data at each shape area grid point $P(x_i, y_i)$ a bilinear interpolation approach is used. To obtain the value at the interpolating point $P(x_i, y_i)$ located inside the shape area having coarser grids, four-point rectangular grid data is identified based on the latitude and longitude values. A One dimensional grid interval along the longitude and latitude direction Δx and Δy respectively is set. where,

$$\Delta x = G(x_1, y_0) - G(x_0, y_0) \tag{2}$$

$$\Delta y = G(x_0, y_1) - G(x_0, y_0) \tag{3}$$

These intervals set the maximum bounding limit for each of the rectangular gridded data. One dimensional linear interpolation along the longitudinal direction is given as

$$Q(x_i, y_0) = \frac{\delta X}{\Delta x}(G(x_1, y_0) - G(x_0, y_0)) + G(x_0, y_0) \tag{4}$$

$$Q(x_i, y_1) = \frac{\delta X}{\Delta x}(G(x_1, y_1) - G(x_0, y_1)) + G(x_0, y_1) \tag{5}$$

These equations of one-dimensional interpolation can be extended to the bilinear interpolation method to get the value at point $P(x_i, y_i)$ as follows

$$\begin{aligned} P(x_i, y_i) &= \frac{\delta Y}{\Delta y}(Q(x_i, y_1) - Q(x_i, y_0)) + Q(x_i, y_0) \\ &= \frac{\delta Y}{\Delta y}\left[\frac{\delta X}{\Delta x}(G(x_1, y_1) - G(x_0, y_1)) + G(x_0, y_1)\right) - \frac{\delta X}{\Delta x}(G(x_1, y_0) - G(x_0, y_0)) + G(x_0, y_0))\right] + \frac{\delta X}{\Delta x}(G(x_1, y_0) - G(x_0, y_0)) + G(x_0, y_0)) \\ &= \frac{\delta X}{\Delta y}\frac{\delta Y}{\Delta y}G(x_0, y_1) + \frac{\delta Y}{\Delta y}\left(1 - \frac{\delta X}{\Delta x}\right)G(x_0, y_1) + \frac{\delta X}{\Delta x}\left(1 - \frac{\delta Y}{\Delta y}\right)G(x_1, y_0) + \left(1 - \frac{\delta X}{\Delta x} - \frac{\delta Y}{\Delta y} + \frac{\delta X}{\Delta x}\frac{\delta Y}{\Delta y}\right)G(x_0, y_0) \end{aligned} \tag{6}$$

The final value at the bilinear interpolation point is independent of the order of the step followed, *i.e.*, if one-dimensional bilinear interpolation along latitude is carried out first followed by the longitudinal direction, the resultant value will be the same.

Thus, the resultant data value for the given shape is given as

$$D(S_A) = \frac{1}{N}\sum_{i=0}^{m}\sum_{j=0}^{n} P(x_i, y_i) \; \forall \; P(x_i, y_j) \in S_A \tag{7}$$

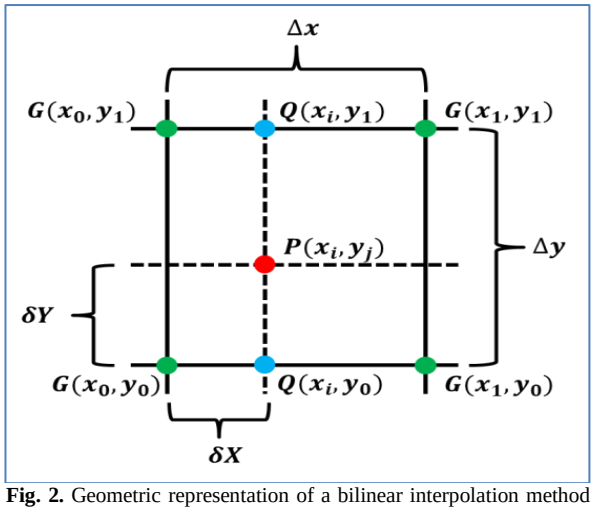

Fig. 2. Geometric representation of a bilinear interpolation method representing the interpolation of shape area points from rectangular gridded data points

where N denotes the total number of points in a given shape area, m and n are the number of coordinate points for x and y directions respectively. Equation 7 gives the data value for the given spatial domain (Sub-division or district) obtained from the mean of interpolated data and associated data points in the given domain.

Bilinear interpolation works as a robust technique for extracting temperature data at sub-division and district levels from coarser grid sizes. The method's validity was assessed by comparing the interpolated data extracted at the sub-division level with the corresponding data of IMD. By leveraging neighboring data points and linear interpolation between them, this method effectively captures spatial variability in temperature, providing more accurate and localized estimates. The method adds advantage to temperature data extraction from the courser grid as the maximum characteristics are preserved in the interpolation method. This ensures that the extracted temperature values maintain the overall trends and variations observed in the broader grid dataset, thereby enhancing the accuracy and reliability of the extracted information.

2.3. *Evaluation matrix*

Statistical measures are used in forecast skill analysis to assess the relationship between observed and forecasted temperature values. The correlation coefficient (CC) technique is used to assess the prediction skill of the model with observation in an extended time period (i.e. week1 to week4 average). The correlation coefficient indicates how well the forecasted temperature values align with the actual observed temperature values. A CC close to 1 indicates a strong positive linear relationship, suggesting high forecast skill, while a coefficient close to

TABLE 1

Contingency table to estimate the frequency of ERF model data with observed data

		Observed Data		
		Yes	No	
ERF Model Data	Yes	Hits (a)	Misses (c)	a+c
	No	False Alarm (b)	Correct Negative (d)	b+d
		a+b	c+d	Total (a+b+c+d)

-1 indicates a strong negative linear relationship. A coefficient near 0 suggests a weak or no linear relationship between the forecast and observed values. For the current research, the CC is calculated using equation 8 as follow (Callaghan, 1996)

$$CC = \frac{\sum_{i=1}^{N}(P_{oi} - P_o)(P_{fi} - P_f)}{\sqrt{\sum_{i=1}^{N}(P_{oi} - P_o)^2}\sqrt{\sum_{i=1}^{N}(P_{fi} - P_f)^2}} \quad (8)$$

where P_{oi} and P_{fi} are the observed and forecasted values at the N number of selected grid points. P_o and P_f are the average values of the observed and forecasted estimations for N values.

The accuracy of model prediction is further evaluated by using the categorical temperature forecast's yes/no nature. The term categorical refers to the fact that the forecast verification is either yes or no. Each verification time is graded in one of four categories: hits (a), false alarms (b), misses (c), or correct negatives (d). The contingency table, for example, depicts the frequency of 'yes' and 'no' projected and actual events, where yes indicates that an event occurred and no indicates that it did not. Table 1 shows the yes and no events that make up a contingency table. Other computations are also performed to evaluate the model's ability to forecast T_{max} and T_{min} during the DJF. Accuracy, Bias, Probability of Detection (POD), False Alarm Ration (FAR), Probability of False Detection (POFD), Critical Success Index (CSI), and Equitable Threat Score are some of the factors to consider (ETS). All of these are calculated using hits, misses, false alarms, and correct negatives, as described in a contingency table. Accuracy (fraction correct) gives what fraction of the forecast was correct. Accuracy ranges from 0.0 to 1.0 with 1.0 as a perfect score (Wilks, 2011).

$$\boldsymbol{ACCURACY} = \frac{Hits(a) + Correct\ Negative(d)}{Total} \quad (9)$$

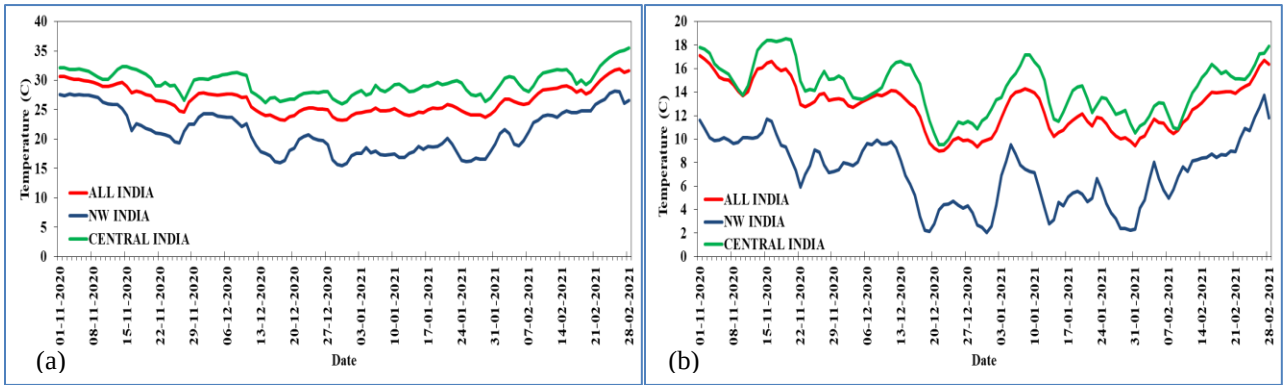

Figs. 3(a&b). Daily observed (a) Maximum temperature average and (b) Minimum temperature average over India as a whole, Northwest India and Central India

The frequency bias or Bias (BIAS) score gives the forecasted frequency of 'yes' events compared to the observed frequency of 'yes' events. Bias score ranges from 0.0 - ∞, with 1.0 as a perfect score. When the bias score is less than 1.0, it indicates that the forecast system tends to under-forecast, while a score greater than 1.0 shows system over-forecasting (Schwartz, 2017)

$$\boldsymbol{BIAS} = \frac{Hits(a) + False\ Alarm(b)}{Hits(a) + Misses\ (c)} \tag{10}$$

Similarly, the probability of detection (POD) corresponds (Wehling *et al.*, 2011) to what fraction of the observed 'yes' events were correctly forecasted. With a perfect score as 1.0, POD ranges from 0.0 to 1.0.

$$\boldsymbol{POD} = \frac{Hits(a)}{Hits(a) + Misses\ (c)} \tag{11}$$

The false alarm ratio (FAR) measures the fraction of the 'yes' forecasted events that did not occur. The FAR value ranges from 0.0 to 1.0, with a perfect score of 0 (Lim et. al., 2019).

$$\boldsymbol{FAR} = \frac{False\ Alarm(b)}{Hits(a) + False\ Alarm(b)} \tag{12}$$

Probability of false detection (POFD) responds to the question of what fraction of the observed 'no' events were incorrectly forecasted as 'yes'. With a perfect score of 0.0, the POFD value ranges from 0.0 to 1 (Wilks, 2011).

$$\boldsymbol{POFD} = \frac{False\ Alarm(b)}{Correct\ Negative(d) + False\ Alarm(b)} \tag{13}$$

The critical success index (CSI) answers the question of how well the forecast 'yes' event corresponds to the observed 'yes' event. The CSI score ranges from 0.0 to 1.0, with 0.0 indicating no skill in the forecast and 1.0 indicating a perfect score (Schaefer, 1990).

$$\boldsymbol{CSI} = \frac{Hits(a)}{Hits(a) + Misses(c) + False\ Alarm(b)} \tag{14}$$

The equitable threat score (ETS) responds to the question of how well the forecast 'yes' event corresponds to the observed 'yes' event. The equitability in ETS allows the score to be compared more fairly across the different categories. The ETS value ranges from -1/3 to 1.0, with a score indicating 0.0 as no skill and 1.0 as a perfect score (Mesinger, 2008).

$$\boldsymbol{ETS} = \frac{Hits(a) + Hits_{Random}}{(Hits(a) + Misses(c) + False\ Alarm(b) - Hits_{Random})} \tag{15}$$

where,

$$\boldsymbol{Hits_{Random}} = \frac{(Hits(a) + Misses(c))(Hits(a) + False\ Alarm(b))}{Total}$$

Figs. 3.a-b represents the daily weighted area average time series calculated by taking the summation of the product of temperature value at sub-divisional level and area weightage to the sum of area weightage for the entire Indian subcontinent, the North-West (NW) landmass, and the Central (CI) landmass. The weighted area average can be given as (Liou, 1992)

$$W_i = \frac{\sum_{j=1}^{n} D(S_A)_j \mathrm{A}_j}{\sum_{j=1}^{n} \mathrm{A}_j} \tag{16}$$

where $D(S_A)_j$ is the data value for the sub-division in the landmass for which the weighted area average be calculated and A_j gives the corresponding area for the sub-division. The daily T_{max} for the area CI continues to

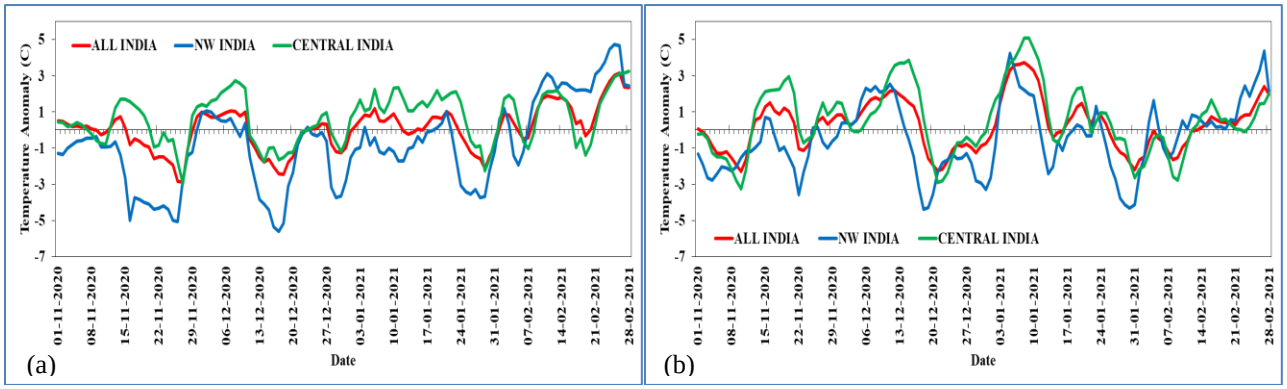

Figs. 4(a&b). Daily anomaly in observation for (a) Tmax and (b) Tmin over India as a whole, Northwest India and Central India

be slightly higher than the whole India average, while the daily T_{max} for NW India continues to be lower than the overall India average. T_{max} was found to be around 5 °C lower during the peak winter days/months (December and January) than during the other months. The fluctuation in T_{max}, on the other hand, follows similar patterns during the entire season across India, the Northwest, and Central India. Also noted over these regions during the first few days and last week of December was an increase in the T_{max}. There is a strong correlation between the arrival of western disturbances and the onset of cold wave conditions across the northern parts of India. Cold air from northern latitudes is transported into India by western disturbances, which appear as eastward-moving, well-marked troughs in the upper troposphere of westerly winds north of 20° N and are frequently observed extending into the lower troposphere.

Further, the departure (or anomaly) in T_{max} and T_{min} are shown in Figs. 4a-b respectively for the country as a whole, NW and CI. During the winter season from November 2020 to February 2021, the maximum temperature remains normal, with the occasional drop-in departure around 2.5 °C during the end of November and mid-December. The Tmin departure during the season can be observed oscillating with a negative temperature anomaly in mid-November, mid-December, and January end with a positive temperature anomaly. In the smaller regional domain of Northwest India, cold wave conditions prevailed with the minimum temperature departure ranging from 3 °C to 4.5 °C between 20-24 November, 18 December – 02 January, and 27-31 January. Figs. 4a shows that the maximum temperature departure for the NW Indian region can be observed below normal condition throughout November-January, followed by the positive departure in maximum temperature. In the case of the Central India region, the minimum and maximum temperature departure closely followed India's departure trend as a region.

From Figs. 4 for the Northwest India region, it can be observed that the long-term drop in maximum temperature departure was followed by a sharp decline in the minimum temperature departure during the season. During 15-26 November, the maximum temperature departure ranges from 3.5° C to 5° C. Similarly, a negative anomaly can be observed during 13-20 December and 24-31 January for maximum temperature. The minimum temperature departure peak can be seen on 22 November, 18 December, and 29 January, showing the peak minimum temperature departure following the long-term peak drop in the maximum temperature departure. The large-scale features associated with these cold waves over the Indo-Gangetic Plains (Northern parts of India) during the winter season of 2020-21 are associated with cold north-westerly winds reaching from the cooler regions of Central Asia/ Hindukush, lowering temperatures over the regions, resulting in cold wave conditions.

3. Results and discussion

3.1. *Minimum Temperature (T_{min}) Bias in ERF during winter season*

IMD prepares temperature forecasts on a weekly basis for extended time periods based on the operational run of CFSv2. However, there is a consistent bias in temperature prediction. The bias in a predictive deterministic model arises from incorrect parameterisation and a lack of sufficient observation of the model's initial conditions. Accurate weather prediction is made considerably more difficult by the presence of systemic biases in the models (Pattanaik *et al.*, 2017a; Kumar *et al.*, 2022). Biases must be reduced using statistical or dynamical methods (post processing) to increase forecast predictability and accuracy (Singh *et al.*, 2020). Bias correction approaches have resulted in significant

changes/improvements in the raw forecast and approach to observation since they reduce the mean error in the

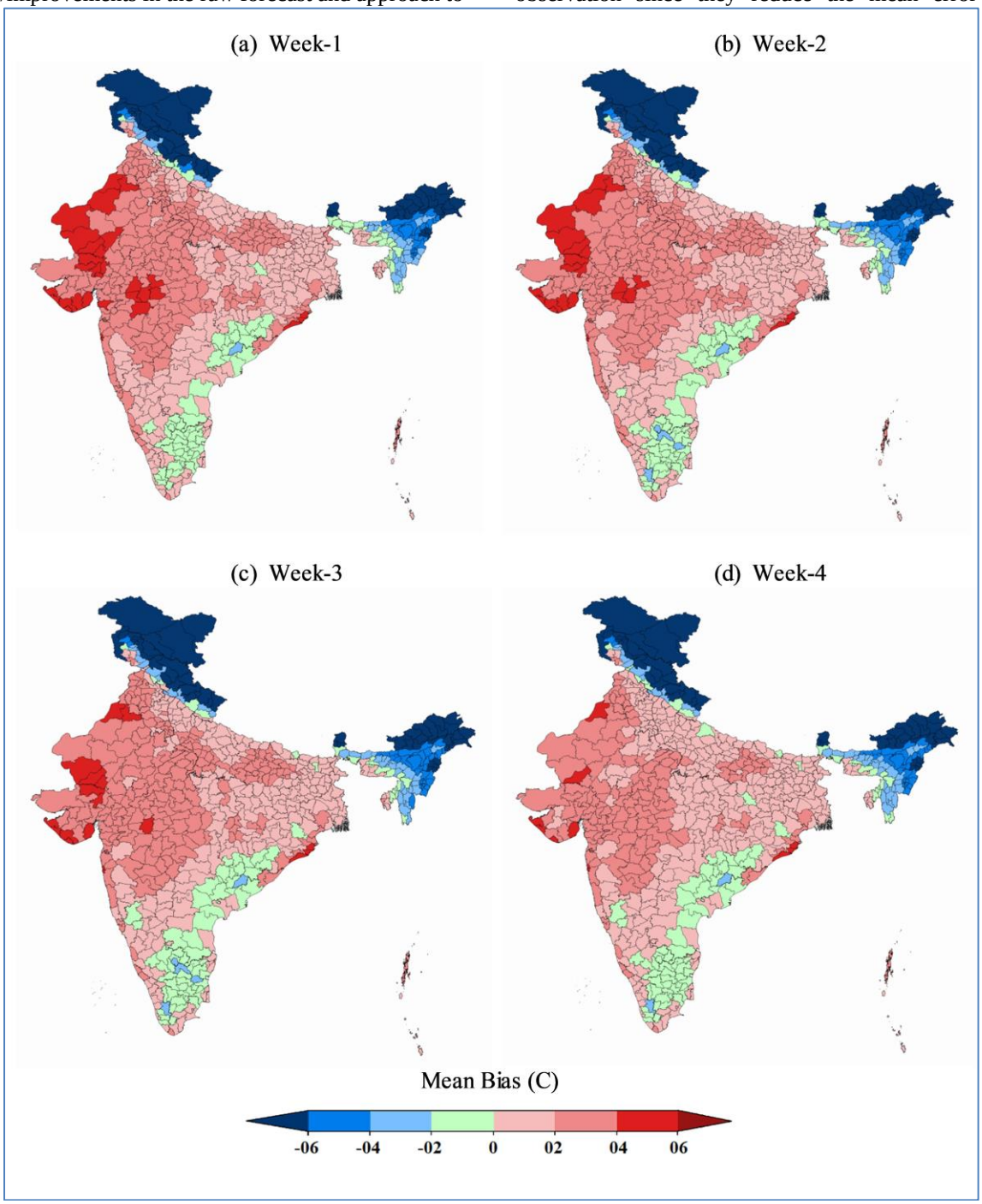

Figs. 5(a-d). Mean Bias for the CFSv2 Tmin forecast for (a) Week-1 (b) Week-2 (c) Week-3 (d) Week-4 for the NDJF period

model's forecast. Richardson's simple mean correction method is a statistical technique used in the context of bias correction for various meteorological and climate variables, particularly temperature and precipitation. It addresses biases or systematic errors present in climate model simulations or observational datasets. The technique used is relatively straightforward and involves correcting biases by adjusting the mean of the model or observed data. It calculates the mean bias (the average difference between model and observed data) and then subtracts or adds this mean bias to each data point in the dataset. The bias can be considerably reduced by post-

processing raw forecast using appropriate techniques. As a result, bias correction is applied to the raw ERF temperature forecast over a 32-day period. The bias-corrected T_{min} forecast was compared to the raw forecast of T_{min} over the districts, as shown in
Figs. 5, to determine the quantitative improvement on a weekly basis. The figure also shows the consistency of negative bias over the Himalayan region and positive bias over the central Indian region over the four-week period. The model forecast shows the general tendency to be very high or very low in this region, which occurs due to the consistent difference in actual temperature and previously generated forecast. (Pattanaik *et al.,* 2017b) The heat wave analysis shows the model bias in T_{max} over extreme north India; northeast India shows negative bias while Gujarat and adjoining northwest India extend south-eastwards along the Indo-Gangetic plain towards Odisha, showing positive bias.

The Himalayan range above the northeast and northwest regions has a negative bias. In contrast, the planes of the central and northwest regions have a positive bias for all four-week raw forecasts, as seen in the figure. It is also worth noting that just a few districts in the eastern south peninsular have a negative bias across the four-week period. Positive bias implies that the raw model forecast has a propensity to under-predict, whereas negative bias suggests that the model forecast has a tendency to over-predict. The large negative bias over the Northeast and western parts of the Himalaya region and positive bias over central India could be due to imperfect model physics, initial conditions and boundary conditions (Hart *et al.,* 2004; Krishnamurti *et al.,* 2004; Durai and Bhradwaj 2014). As shown in
Figs. 5, the CFSv2 model has to be corrected for this bias. Richardson's simple mean correction approach is utilised to reduce model temperature forecast biases in this study (Richardson 2001).

3.2. *Performance of real time ERF of minimum temperature (T_{min}) during winter 2020-2021.*

Fig. 6(a-c) depicts the weekly T_{min} in observation and ERF forecast for different initial conditions (IC) for a four-week lead time (week 1 to week 4) for all India, NW, and CI. It is worth noting that the ERF forecast accurately predicted the intra-seasonal drop in minimum temperature during the winter period of 18-24 December and 25-31 December 2020. ERF closely captures the trends in Tmin with the observed minimum temperature over the four-week forecast period during the entire season for the NW India of the homogeneous region (Fig. 6b). Fig. 6c depicts the trend of T_{min} (weekly average) during the winter season 2020-2021, which is well below the ERF model forecast. Similarly, to the forecasts for all of India as a homogeneous region, both the Northwest and Central India homogeneous regions show a close correlation during the week beginning December 18th and ending December 25th, 2020.

3.3. *ERF skill of Tmin at meteorological sub-division and homogeneous regions*

The spatial correlation coefficient for T_{min} between ERF and IMD observations are calculated and presented in Figs. 7 for week1 to week4 over meteorological sub-divisions of India. It is observed that the week1 CC for the meteorological sub-division's ranges from 0.72 to 0.97. In the subsequent week period *i.e*. during week2 to week4, the CC is reduced to 0.32-0.93, 0.36-0.88, and 0.11-0.93, respectively over the regions of met sub-division. The CC for W1 and W2 shows high significance and W3 shows moderate. Although the CC for week4 is positive, it is not significant for the forecasting. During the week1, the north-west, central, eastern and north-eastern parts of met-subdivisions have the highest CC (more than 0.9). Fig. 7 shows a sudden loss in forecast skills over the southern peninsular region of India. As seen in Figs. 4 (a & b), there is an oscillation in maximum and minimum temperature anomaly to the mean over the repetitive duration of two weeks. This anomaly shift in weather is poorly forecasted by the model over these regions with longer lead time. Also, it can be seen from figure 6 that although the NW and CI regions show a considerably high correlation between week3 and week4 forecasts, with the poor performance of the model in the southern peninsular region over India.

Fig. 8 shows the CC for all India, along with the homogeneous region of NW and CI. The week1 forecast shows high CC for all three domains and is found to be above 0.9. During the winter, the minimum temperature forecast is consistent with observations throughout the season over the northwest and central regions of India. The north-westerly wind, in conjunction with the anti-cyclonic circulation that continues up to the middle of the troposphere, does help in maintaining the minimum temperature at a level that is below (colder) and uniformly distributed across the regions at this particular time. A gradual fall in the CC can be observed beyond the week2 period. In the case of the NW India of the homogeneous region, the CC value drops till week3, showing a further increase in the CC value in week4. Since the temporal variability in T_{min} is noticed, and deflection is supported largely owing to the approach of Western Disturbance over the regions, and since these are infrequent phenomena, therefore, prediction becomes non reachable due to weak models' parameterizations. In the case of the CI, a significant reliable CC is observed up-to the week3 period. A poor CC is observed for CI in week4. The same

can be reflected through the meteorological sub-division, showing the high CC for the Northwest regional sub-

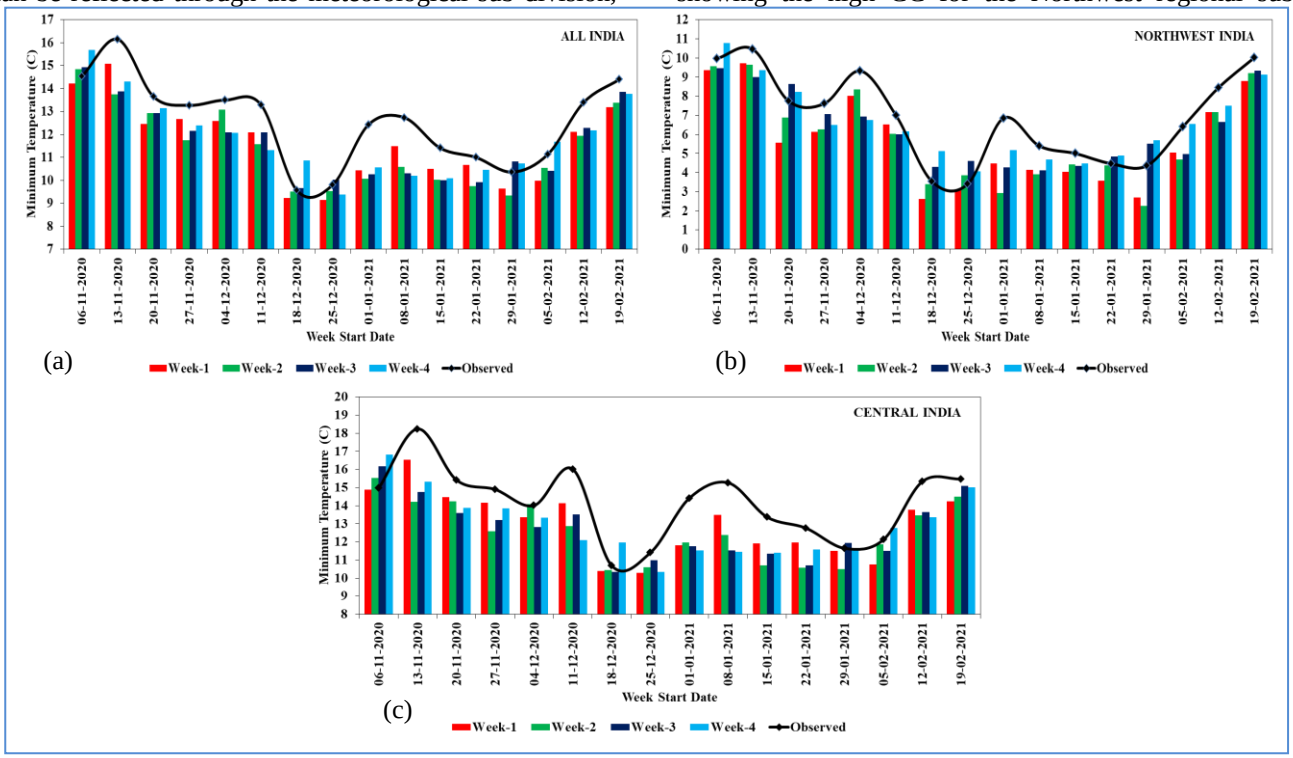

Figs. 6(a-c). ERF four week forecast and the observed weekly minimum temperature for (a) All over India (b) Northwest India and (c) Central India

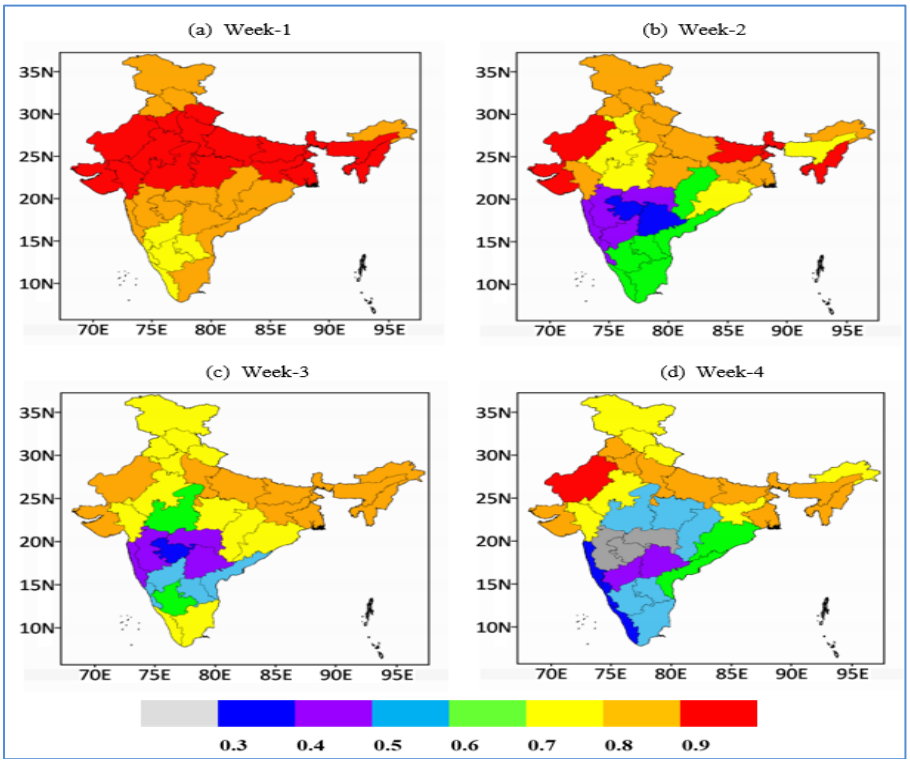

Figs. 7(a-d). Observed and ERF forecasted minimum temperature correlation coefficient for the winter season (NDJF 2020-21) over the meteorological sub-divisions for (a) Week-1 (b) Week-2 (c) Week-3 and (d) Week-4

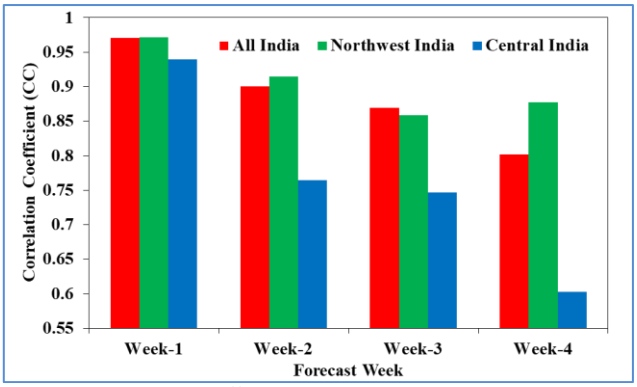

Fig. 8. Correlation coefficient (CC) between observed and ERF forecasted minimum temperature during the winter seasons 2020-21

divisions over the all four-week period and higher correlation up to three weeks in the case of the Central region sub-divisions. Thus, although the Indian domain, two homogeneous regions, and meteorological sub-divisions show a positive correlation, the ERF forecast over the three weeks shows the usefulness to the users.

3.4. *Categorical and quantitative skill analysis over the district domain*

To determine categorical and quantitative capabilities, an assessment of the Indian domain's whole districts (676) is conducted. The weeks of 06-12 Nov 2020, 18-24 Dec 2020, and 29 Jan-04 Feb 2021 are considered to investigate the association between observed and ERF projected T_{min} (**Error! Reference source not found.**). **Error! Reference source not found.**(a) depicts the cold weather conditions during the early winter season, with considerably below normal minimum temperatures, in all three forecasted weeks over the districts of the Jammu and Kashmir sub-division, as well as both homogenous regions of Northwest and Central India. The cold wave situation prevailed in the northern part of India throughout the target week 18-24 December 2020, as indicated in **Error! Reference source not found.**(b), and its ERF forecasting was well ahead of schedule with IC 02 December 2020. The active phase of a cold wave that was expected to pass over Northwest and Central India from 29 January to 4 February 2021 in the ERF was successfully captured with 2-3 weeks lead time (Fig. 9c). The extreme negative anomaly and the propagation of cold winds were both accurately represented by the ERF for the minimum temperature over the next three weeks, which was based on the IC for January 13, 2021. The north westerly wind that brings cold air over the NW and CI is very well captured. The categorical skill score for India's 676 districts, 179 districts in Central India, and 203 districts in Northwest India is shown in **Error! Reference source not found.**.

The measured lowest temperature over the district domain level is categorically analysed with minimum temperature anomalies less than -2 in the Below Normal (BN) / Appreciably Below Normal category, -2 to +2 in the Normal (N) category, and greater than +2 in the Above Normal (AN)/ Appreciably Above Normal category. The accuracy plot for India, Central India, and Northwest India indicates excellent accuracy in the above normal and below normal categories, but low accuracy forecast skills in the normal category. The above-normal category temperature is under forecasted in all three homogeneous regions, while it is well predicted in the normal region with over forecasted with the 4th week prediction. The below-normal category depicts over predicting for the first two weeks, followed by under forecasting for all of India and the homogenous parts of Northwest India.

The POD plots in **Error! Reference source not found.** give the relative operating characteristics of the forecast. The POD value is high for the N and BN categories, while the detection probability is at least in the AN range. In all three categories, with the change in forecast week, detection probability is seen to be decreasing. **Error! Reference source not found.** shows the FAR indicating the fraction of ERF forecasted events that did not occur in the observations. From the figure, it can be observed that the normal category shows the least false alarms as compared to other categories, with the below normal category showing maximum false alarms. In order to find the probability of false alarm rate, POFD is shown in figure indications the good score in above normal and below the normal range and least score in the normal range with an increase in forecast week. Threat score or CSI, shows that more than half of the minimum temperature forecast events were correctly forecasted compared to AN and BN category. The BN category shows comparatively higher forecast events correct for the BN category than AN category. ETS corresponding to the forecasted true events to the observed true events are shown in the figure. The ETS score shows the higher skills in the below normal category as compared to others. It also depicts the better skill in week one forecast over the week four in all three categories.

4. Summary and conclusion

Temperature plays an essential role in a wide range of applications, and it is particularly important in agriculture, power sector, human health, tourism and other sectors. Minimum temperature (T_{min}), on the other hand, is extremely important throughout the winter since it gets translated into cold waves and cold days. IMD runs an operational CFSv2model every week for the ERF (Forecast up to 4 weeks) of T_{min} and disseminates it to different stakeholders for sectorial applications. As a

result, we must investigate and evaluate the model's reliability in simulating T_{min} over the landmass of India. Therefore, we carry out the present investigation. The

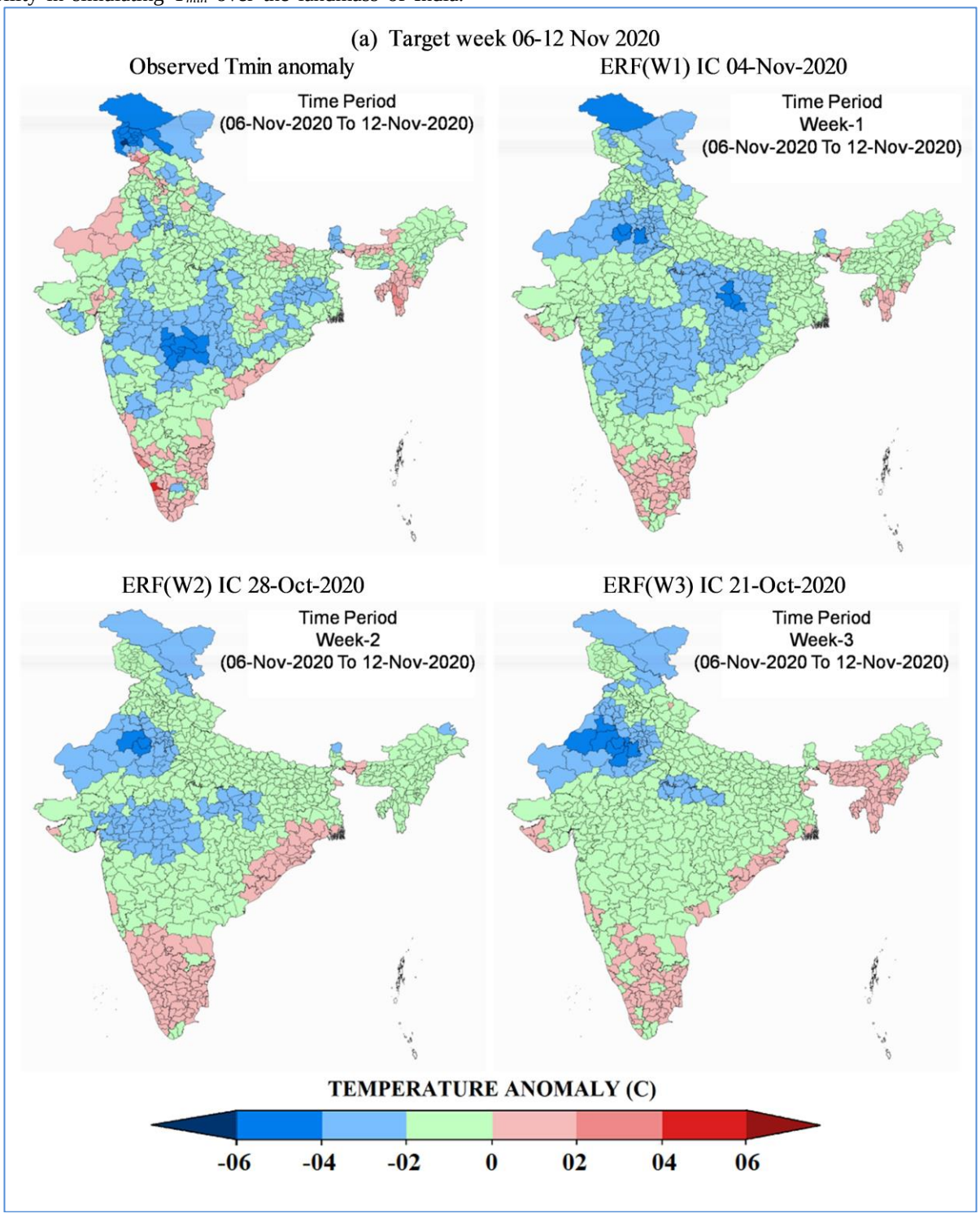

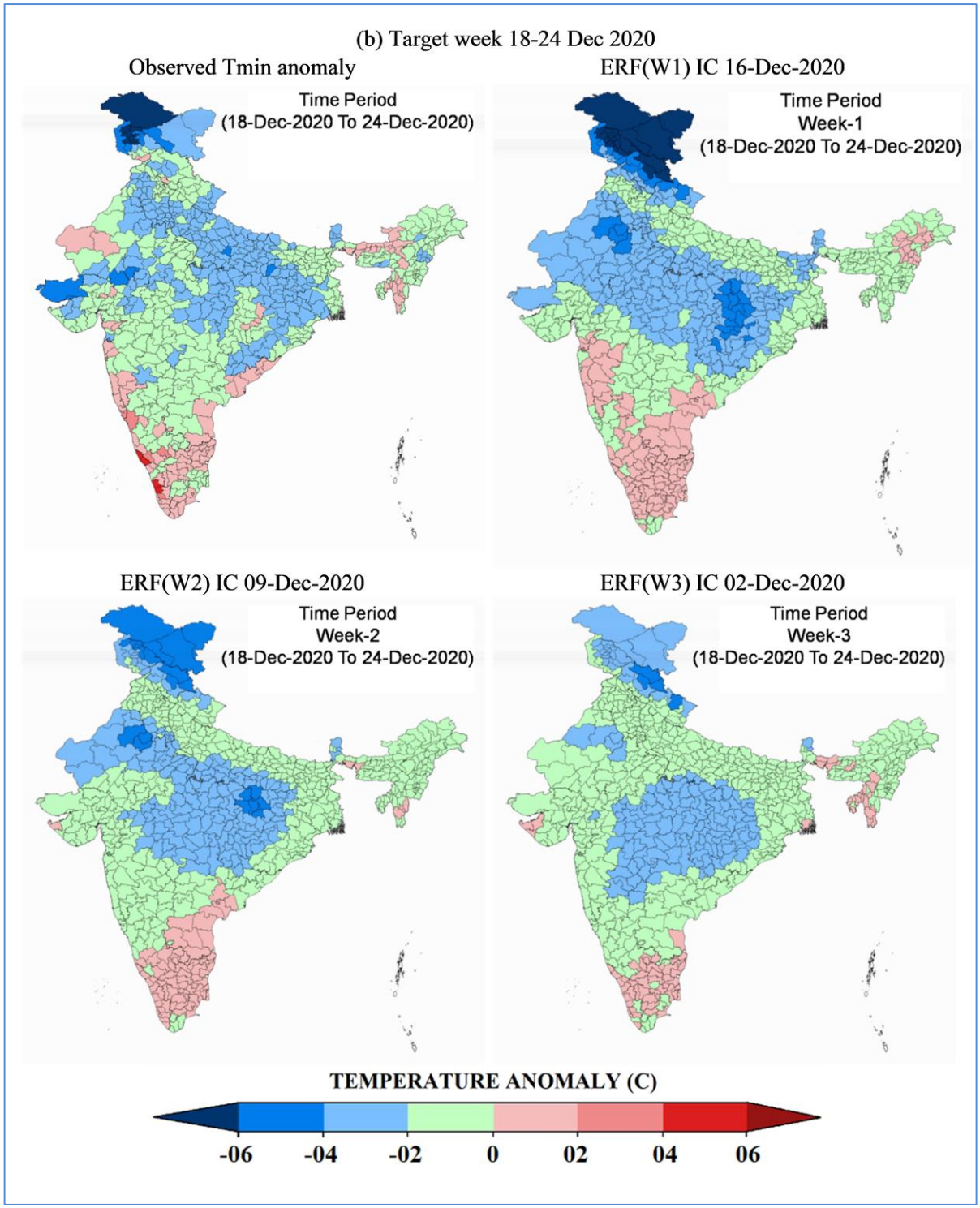
(b) Target week 18-24 Dec 2020
Observed Tmin anomaly
Time Period
(18-Dec-2020 To 24-Dec-2020)
ERF(W1) IC 16-Dec-2020
Time Period
Week-1
(18-Dec-2020 To 24-Dec-2020)
ERF(W2) IC 09-Dec-2020
Time Period
Week-2
(18-Dec-2020 To 24-Dec-2020)
ERF(W3) IC 02-Dec-2020
Time Period
Week-3
(18-Dec-2020 To 24-Dec-2020)
TEMPERATURE ANOMALY (C)
-06
-04
-02
0
02
04
06

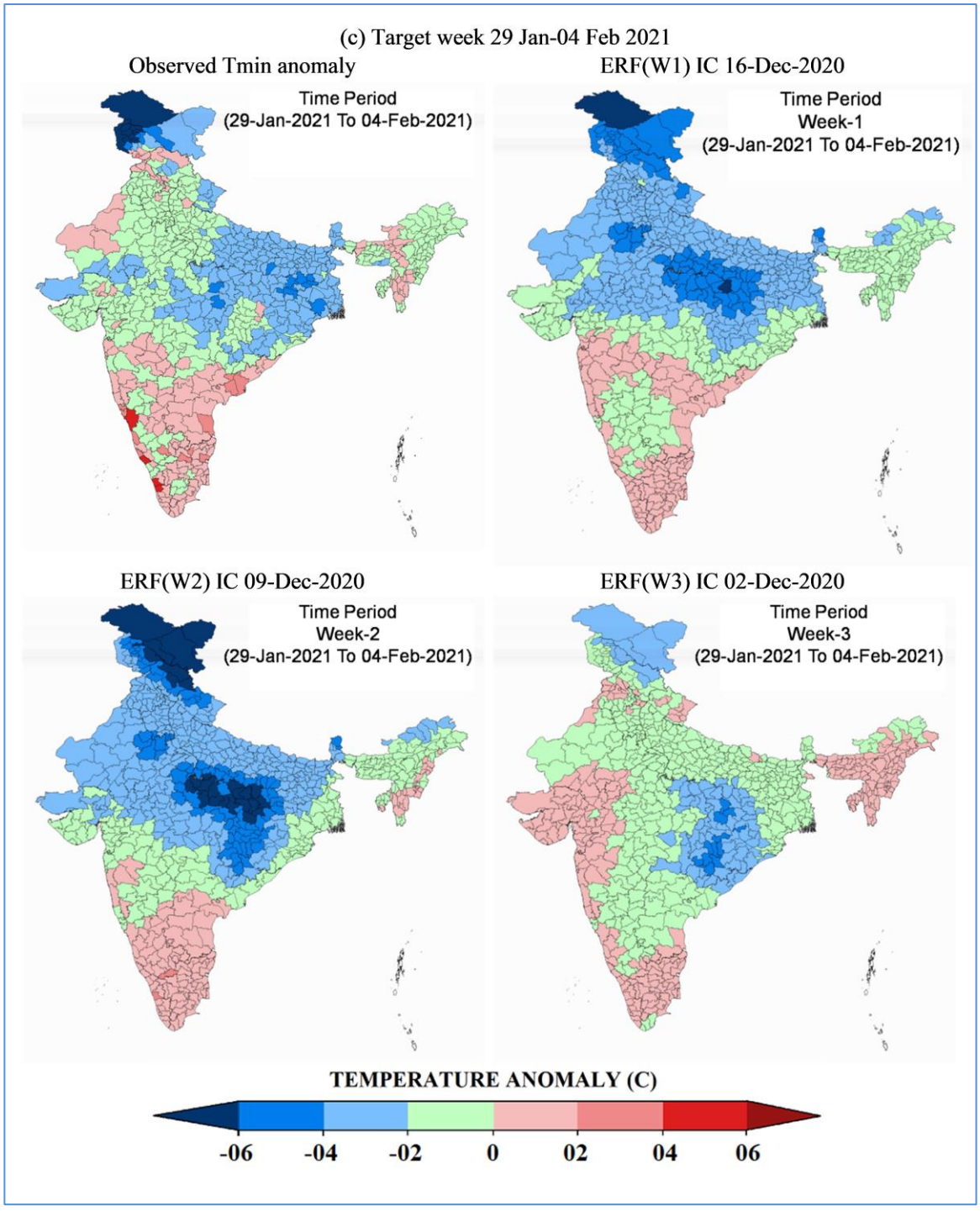

Figs. 9(a-c). Observed weekly minimum temperature anomaly and three weeks ERF minimum temperature anomaly for the same target week (a) 06-12 Nov 2020 (b) 18-24 Dec 2020 (c) 29 Jan-04 Feb 2021

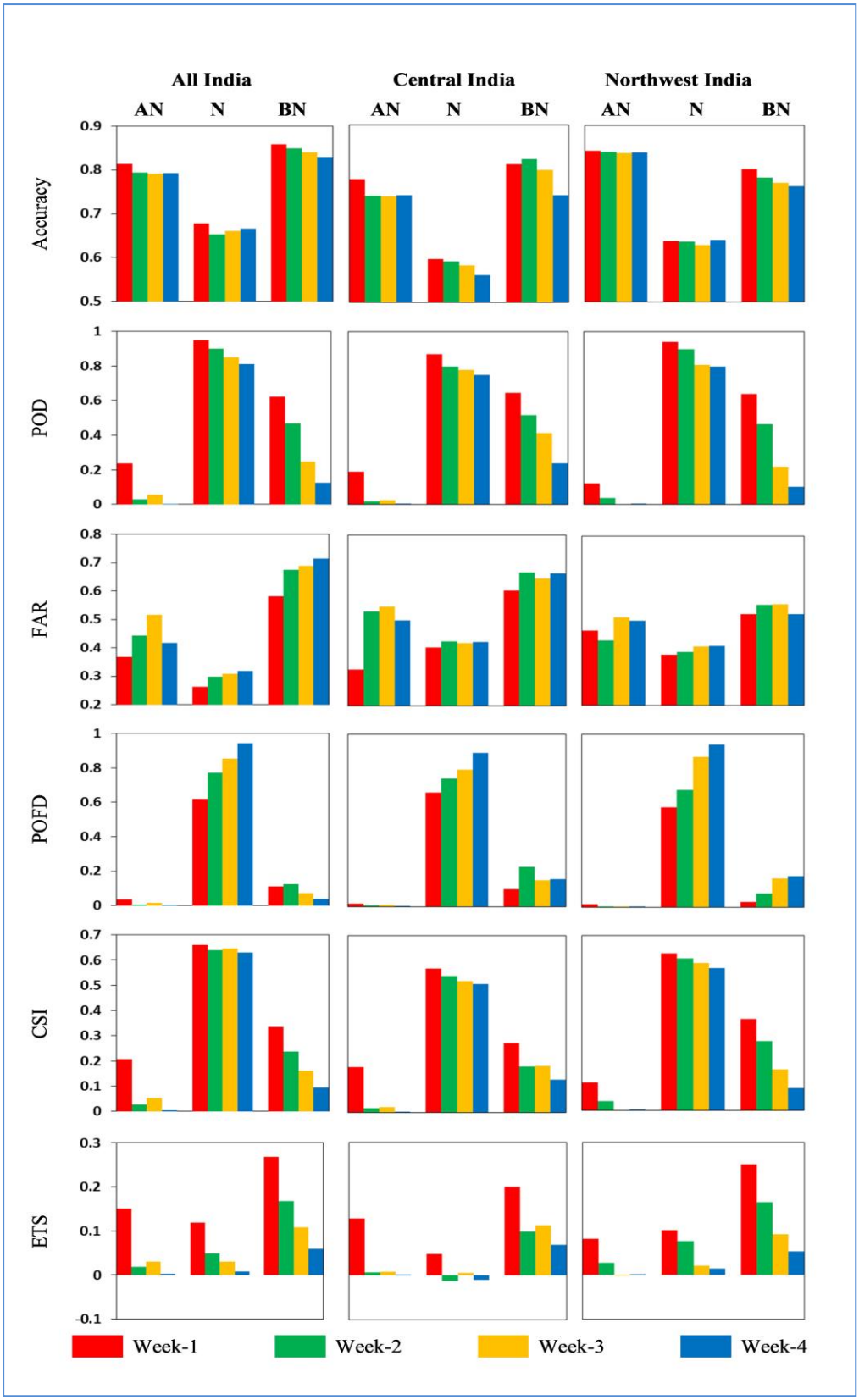

Fig. 10. Categorical skill score of ERF minimum temperature forecast overall India, Central India and Northwest India

quantitative and categorical skill analysis is carried out over India's temperature homogenous areas, meteorological sub-divisions and smaller geographical district domains. The skills are evaluated based on the forecast performance of each week for the T_{min} predictions for the next four weeks based on the operational ERF. It is realised that the observed variability of T_{min} in the observation is very well predicted in the ERF forecast. However, the model has some biases (positive bias) and it is slightly over-predicting the below-normal temperature for the homogeneous regions. Thus, the operational forecast is prepared with bias correction. The results reveal that ERF has better performance and reflects significant skill for periods of up to three weeks during the winter season of 2020-21. It is relatively challenging to make an extended-range forecast, which bridges the gap between medium-range and seasonal forecasts. The ERF is comparatively difficult, as much memory of the initial atmospheric conditions is lost, and this may result in decreased skill at predicting rainfall amounts during W3 to W4. The representation of better physics and parameterization could enhance the skill in predicting the T_{min} in model simulations. The quantitative forecast skill analysis performed over the meteorological sub-division have indicated a significant correlation coefficient between ERF T_{min} with that of observed T_{min} over the meteorological subdivisions of northwest and central India.

The categorical forecast skill of T_{min} forecasts in terms of prediction Above Normal, Normal and Below Normal at the district level was analysed in detail using the verification scores Accuracy, POD, FAR, POFD, CSI, and the ETS values. The accuracy of the forecast four weeks in the three category domains of Above normal, Normal and Below Normal ranges from 0.81 to 0.79, 0.67 to 0.65 and 0.85 to 0.83, respectively, indicating higher accuracy in the case of below normal and above normal cases compared to that of the normal categories. With regard to the biases, it is relatively low in the normal and below normal categories, whereas it is slightly higher in the above normal category showing an over forecasting tendency. The ETS score shows the higher skills in the below normal category as compared to others. It also depicts the better skills in week one forecast over the week four in all three categories. Thus, these results show that ERF has good skill over minimum temperature forecasting with about three-week in advance over the smaller spatial domains of meteorological sub-divisions and smaller spatial scale at district level.

Climate systems vary seasonally due to El Nino, La Nina, and other large-scale climatic trends. The findings from one year help us understand how coupled models perform within the changing climate system. This research emphasizes extreme weather events to demonstrate the ERF model's usefulness and reliability in forecasting these.

Availability of data and material/ Data availability

The data may be available upon genuine request.

Funding

There is no funding for current research

Conflicts of interest

The authors declare no competing interests.

Ethics approval/declarations

Not applicable

Consent to participate

Not applicable

Consent for publication

All authors consent to publish the research.

Acknowledgement

The listed authors are highly grateful to the India Meteorological Department for providing the real time extended range forecast data through the collaborative efforts of IITM, NCMRWF, INCOIS and NCEP institutes of the MoES. The authors are also thankful to the Director General of Meteorology Dr. M. Mohapatra for his encouragement and providing the all required facilities.

Authors' Contributions

Ashish Alone: Conceptualized and analysis as well as the writing of the manuscript.
D. R. Pattanaik: conceptualized (Email-drpattanaik@ gmail.com)
Praveen Kumar: conceptualized, analysis as well as the writing of the manuscript. (Email-praveen221288@ gmail.com)
Anoop Kumar Shukla: conceptualized (Email- akshukla1 @amity.edu).

The manuscript was looked over by all of the authors. All authors made an equal contribution.

Disclaimer: The contents and views presented in this research article/paper are the views of the authors and do

not necessarily reflect the views of the organizations they belong to.

References

Andrews, H. C. and Patterson, C. L., 1976, "Digital interpolation of discrete images", *IEEE Transactions on Computers*, **100**, 2, 196–202.

Bedi, H. S. and Parthasarathy, B., 1967, "Cold Waves over northwest India and neighbourhood", *Mausam*, **18,** 3, 371-378.

Bhatla, R., Gupta, P., Tripathi, A. and Mall, R. K., 2016, "Cold Wave/Severe Cold Wave Events during Post-Monsoon and Winter Season over Some Stations of Eastern Uttar Pradesh, India", *Journal of Climate Change*, **2**, 1, 27–34.

Callaghan, K., 1996, "The correlation coefficient", *Explorations in College Algebra: Discovering Databased Application*, 553–557.

Dimri, A. P. and Chevuturi, A., 2016, "Western Disturbances – Impacts and Climate Change", Western Disturbances - An Indian Meteorological Perspective, *Cham: Springer International Publishing*, 113-127.

Dimri, A. P., Niyogi, D., Barros, A. P., Ridley, J., Mohanty, U. C., Yasunari, T. and Sikka, D. R., 2015, "Western Disturbances: A review", *Reviews of Geophysics*, **53**, 2, 225–246.

Durai, V. R. and Bhradwaj, R., 2014, "Evaluation of statistical bias correction methods for numerical weather prediction model forecasts of maximum and minimum temperatures", *Natural Hazards*, **73**, 3, 1229–1254.

Gupta, P., Bhatla, R., Payra, S., Yadava, P. K. and Verma, S., 2018, "Cold Wave and Severe Cold Wave Events Over Indo-Gangetic Plain : Analysis and Comparison for Decadal Variability", **05**, 02, 101–109.

Hart, K. A., Steenburgh, W. J., Onton, D. J. and Siffert, A. J., 2004, "An Evaluation of Mesoscale-Model-Based Model Output Statistics (MOS) during the 2002 Olympic and Paralympic Winter Games", *Weather and Forecasting*, **19**, 2, 200–218.

Joseph, S., Sahai, A. K., Phani, R., Mandal, R., Dey, A., Chattopadhyay, R. and Abhilash, S., 2019, "Skill evaluation of extended-range forecasts of rainfall and temperature over the meteorological subdivisions of India", *Weather and Forecasting*, **34**, 1, 81–101.

Krishnamurti, T. N., Sanjay, J., Mitra, A. K. and Vijaya Kumar, T. S. V., 2004, "Determination of Forecast Errors Arising from Different Components of Model Physics and Dynamics", *Monthly Weather Review*, **132**, 11, 2570–2594.

Kumar, P., Pattanaik, D. R. and Alone, A., 2022, "Bias-Corrected Extended-Range Forecast Over India for Hydrological Applications During Monsoon 2020", *Pure and Applied Geophysics*, 2018.

Lang, T. J. and Barros, A. P., 2004, "Winter storms in the central Himalayas", *Journal of the Meteorological Society of Japan*, **82**, 3, 829–844.

Lim, J. R., Liu, B. F. and Egnoto, M., 2019, "Cry wolf effect? Evaluating the impact of false alarms on public responses to tornado alerts in the southeastern United States", *Weather, climate, and society*, **11**, 3, 549-563.

Liou, T. S. and Wang, M. J. J., 1992, "Fuzzy weighted average: an improved algorithm", *Fuzzy sets and systems*, **49**, 3, 307-315.

Mandal, R., Joseph, S., Sahai, A. K., Phani, R., Dey, A., Chattopadhyay, R. and Pattanaik, D. R., 2019, "Real time extended range prediction of heat waves over India", *Scientific Reports*, **9**, 1, 1–11.

Mesinger, F., 2008, "Bias adjusted precipitation threat scores", *Advances in Geosciences*, **16**, 137-142.

Midhuna, T. M., Kumar, P. and Dimri, A. P., 2020, "A new Western Disturbance Index for the Indian winter monsoon", *Journal of Earth System Science*, **129, 1**, 59.

NSO 2021. EnviStats-India 2021: Vol. I: Environment Statistics, National Statistical Office, Ministry of Statistics and Programme Implementation, Government of India, New Delhi

Pattanaik, D. R., 2015, "Operational Extended Range Forecast Activity in IMD and its Applications in Different ABSTRACT".

Pattanaik, D. R., Alone, A., Kumar, P., Phani, R., Mandal, R. and Dey, A., 2022, "Extended-range forecast of monsoon at smaller spatial domains over India for application in agriculture", *Theoretical and Applied Climatology*, **147,** 1–2, 451–472.

Pattanaik, D. R., Mandal, R., Phani, R., Dey, A., Chattopadhyay, R., Joseph, S. and Mohapatra, M., 2021, "Large-scale features associated with excess monsoon rainfall over India during 2019 and the real-time extended range forecast", *Meteorology and Atmospheric Physics*, **133**, 4, 1275–1297.

Pattanaik, D. R., Mohapatra, M., Srivastava, A. K. and Kumar, A., 2017a, "Heat wave over India during summer 2015: an assessment of real time extended range forecast", *Meteorology and Atmospheric Physics*, **129**, 4, 375–393.

Pattanaik, D. R., Mohapatra, M., Srivastava, A. K. and Kumar, A., 2017b, "Heat wave over India during summer 2015: an assessment of real time extended range forecast", *Meteorology and Atmospheric Physics*, **129**, 4, 375–393.

Pattanaik, D. R. and Sahai, A. K., 2018, "Evaluation of Real-Time Extended Range Forecast (ERF) of southwest monsoon, heat wave, cold wave, cyclogenesis and northeast monsoon during 2017", *No. ESSO/IMD/NWP-Extended Range Forecast (ERF) Report*, **2018**, 01, 05.

Pattanaik, D. R., Sahai, A. K., Mandal, R., Phani Muralikrishna, R., Dey, A., Chattopadhyay, R. and Mishra, V., 2019, "Evolution of operational extended range forecast system of IMD: Prospects of its applications in different sectors", *Mausam*, **70**, 2, 233–264.

Pattanaik, D. R., Sahai, A. K., Muralikrishna, R. P., Mandal, R. and Dey, A., 2020, "Active-Break Transitions of Monsoons Over India as Predicted by Coupled Model Ensembles", *Pure and Applied Geophysics*, **177**, 9, 4391-4422.

Raghavan, K., 1967, "A climatological study of severe cold waves in India", *Indian J. of Meteorol. Geophys.*, **18**, 1, 91–96.

Rajeevan, M., Rohini, P., Nair, S. A., Tirkey, S., Goswami, T. and Kumar, N., 2023, "Heat and cold waves in india processes and predictability", *IMD Met. Monograph: MoES/IMD/Synoptic Met/01 (2023)/28*, **28**, 26-128.

Ray, K., Giri, R. K., Ray, S. S., Dimri, A. P. and Rajeevan, M., 2021, "An assessment of long-term changes in mortalities due to extreme weather events in India: A study of 50 years' data, 1970–2019", *Weather and Climate Extremes*, **32**, 100315.

Richardson, D. S., 2001, "Ensembles using multiple models and analyses", *Quarterly Journal of the Royal Meteorological Society*, **127**, 575, 1847–1864.

Saha, S., Moorthi, S., Wu, X., Wang, J., Nadiga, S., Tripp, P. and Becker, E., 2014, "The NCEP Climate Forecast System Version 2", *Journal of Climate*, **27**, 6, 2185–2208.

Samra, J. S., Singh, G. and Ramakrishna, Y., 2003, "Cold wave of 2002-03: Impact on agriculture", December, 1–62.

Schaefer, J. T., 1990, "The critical success index as an indicator of warning skill", *Weather and forecasting*, **5**, 4, 570-575.

Schwartz, C. S., 2017, "A Comparison of Methods Used to Populate Neighborhood-Based Contingency Tables for High-Resolution Forecast Verification", *Weather and Forecasting*, **32**, 2, 733–741.

Singh, H., Dube, A., Kumar, S. and Ashrit, R., 2020, "Bias correction of maximum temperature forecasts over India during March–May 2017", *Journal of Earth System Science*, **129**, 1, 13.

Srivastava, A. K., Rajeevan, M. and Kshirsagar, S. R., 2009, "Development of a high resolution daily gridded temperature data set (1969-2005) for the Indian region", *Atmospheric Science Letters*, **10**, 4, 249-254.

Subbaramayya, I. and Rao, D. S., 1976, "Heat wave and cold wave days in different states of India", *Mausam*, **27**, 4, 436-440.

Wehling, P., LaBudde, R. A., Brunelle, S. L. and Nelson, M. T., 2011, "Probability of detection (POD) as a statistical model for the validation of qualitative methods", *Journal of AOAC International*, **94**, 1, 335-347.

Wilks, D. S., 2011, "Statistical methods in the atmospheric sciences", (Vol. 100). *Academic press*.

Zhang, T. and Kumar, A., 2024, "On the Role of Indian Ocean SST in Influencing the Differences in Atmospheric Variability Between 2020–2021 and 2021–2022 La Niña Boreal Winters", *Geophysical Research Letters*, **51**, 5.